PHYSICAL REVIEW D, VOLUME 62, 051502(R)

Systematics of $q\bar{q}$ states in the (n,M^2) and (J,M^2) planes

A. V. Anisovich, V. V. Anisovich, and A. V. Sarantsev
St. Petersburg Nuclear Physics Institute, Gatchina, 188350, Russia

(Received 13 March 2000; published 25 July 2000)

In the mass region up to $M<2400$ MeV we systematize mesons on the plots (n,M^2) and (J,M^2), thus setting their classification in terms of $n^{2S+1}L_J\, q\bar{q}$ states. The trajectories on the (n,M^2) plots are drawn for the following (IJ^{PC}) states: $a_0(10^{++})$, $a_1(11^{++})$, $a_2(12^{++})$, $a_3(13^{++})$, $a_4(14^{++})$, $\pi(10^{-+})$, $\pi_2(12^{-+})$, $\eta(00^{-+})$, $\eta_2(02^{-+})$, $h_1(01^{+-})$, $\omega(01^{--})/\varphi(01^{--})$, $\rho(11^{--})$, $f_0(00^{++})$, $f_2(02^{++})$. All trajectories are linear, with nearly the same slopes. At the (J,M^2) plot we set out meson states for leading and daughter trajectories: for π, ρ, a_1, a_2 and P'.

PACS number(s): 14.40.−n, 12.38.−t, 12.39.Mk

In the last decade a tremendous amount of effort has been made to study meson spectra over the mass region 1000–2400 MeV. The collected rich information that includes the discovery of new resonances and confirmation of those already discovered needs to be systematized.

We present a scheme for the $q\bar{q}$ trajectories on the (n,M^2) and (J,M^2) plots (n is the radial quantum number and J is the meson spin) using the latest results [1–6] together with previously accumulated data [7].

The trajectories on the (n,M^2) plots are presented in Figs. 1 and 2: they are linear and with a good accuracy can be represented as

$$M^2=M_0^2+(n-1)\mu^2. \tag{1}$$

M_0 is the mass of basic meson and μ^2 is the trajectory slope parameter: μ^2 is approximately the same for all trajectories: $\mu^2=1.25\pm0.15$ GeV^2.

At $M\leqslant 2400$ MeV the mesons of $q\bar{q}$ nonets $n^{2S+1}L_J$ fill in the (n,M^2) trajectories as follows:

$$\begin{aligned}
&{}^1S_0\to\pi(10^{-+}),\quad \eta(00^{-+}),\\
&{}^3S_1\to\rho(11^{--}),\quad \omega(01^{--})/\varphi(01^{--});\\
&{}^1P_1\to b_1(11^{+-}),\quad h_1(01^{+-}),\\
&{}^3P_J\to a_J(1J^{++}),\quad f_J(0J^{++})\quad J=0,1,2;\\
&{}^1D_2\to\pi_2(12^{-+}),\quad \eta_2(02^{-+}),\\
&{}^3D_J\to\rho_J(1J^{--}),\quad \omega_J(0J^{--})\quad J=1,2,3;\\
&{}^1F_3\to b_3(13^{+-}),\quad h_3(03^{+-}),\\
&{}^3F_J\to a_J(1J^{++}),\quad f_J(0J^{++})\quad J=2,3,4.
\end{aligned} \tag{2}$$

Trajectories with the same IJ^{PC} can be created by different orbital momenta with $J=L\pm1$; in this way they are doubled: these are trajectories $(I1^{--})$, $(I2^{++})$, and so on.

Isoscalar states are formed by the two light flavor components, $n\bar{n}=(u\bar{u}+d\bar{d})/\sqrt{2}$ and $s\bar{s}$. Likewise, this also results in doubling isoscalar trajectories.

The trajectories $a_1(11^{++})$ and $a_3(13^{++})$ are shown in Fig. 1a: the states $a_1(2100)$, $a_1(2340)$, $a_3(2070)$, $a_3(2310)$ have been seen in [1]; evidence for $a_1(1640)$ was found in [2].

Figure 1b displays the trajectories $\eta(00^{-+})$ and $\eta_2(02^{-+})$: the doubling is due to two independent flavor components $n\bar{n}$ and $s\bar{s}$. The states $\eta_2(2030)$ and $\eta_2(2300)$ have been seen in the analysis [4]. Linear extrapolation of trajectories predicts the mesons $\eta(1900)$, $\eta(2100)$ and $\eta_2(2200)$.

Two trajectories $\rho(11^{--})$ related to S and D $q\bar{q}$ waves are demonstrated in Fig. 1c. The states $\rho(1700)$ and $\rho(2150)$ are cited in [7]; the trajectories predict $\rho(1830)$, $\rho(2060)$ and $\rho(2380)$.

In Fig. 1d one can see the trajectories for 10^{-+} and 12^{-+}. The states $\pi(1300)$, $\pi(1800)$ and $\pi_2(1670)$ are from [7]; all other states are predicted by the linearity of trajectories.

For the $h_1(01^{+-})$ states, two trajectories are shown in Fig. 1e; the states $h_1(2000\pm25)$ and $h_1(2270\pm20)$ are seen in [8].

In Fig. 1f, the $\omega(01^{--})/\varphi(01^{--})$ trajectories are demonstrated; the resonances $\omega(1920\pm40)$, $\omega(2140\pm25)$ and $\omega(2305\pm60)$ are from [8].

Experimental data in the sector $a_0(10^{++})$, $a_2(12^{++})$, $a_4(14^{++})$ do not fix the slope μ^2 uniquely. In Fig. 2a the trajectories $a_0(10^{++})$, $a_2(12^{++})$ and $a_4(14^{++})$ are shown for $\mu^2=1.38$ GeV^2. The states $a_0(2000^{+50}_{-100})$, $a_2(1980)$, $a_2(2100)$, $a_2(2280)$, $a_4(2005)$, $a_4(2260)$ have been observed in [1,3] and $a_2(1640\pm60)$ in [9]. Two trajectories $a_2(12^{++})$ owe their existence to two states, ${}^3P_2 q\bar{q}$ and ${}^3F_2 q\bar{q}$. Obviously, the upper one refers to states with dominant ${}^3F_2 q\bar{q}$ component. In Fig. 2b one can see the trajectories $a_0(10^{++})$, $a_2(12^{++})$, $a_4(14^{++})$ for $\mu^2=1.1$ GeV^2. Comparison of Figs. 2a and 2b demonstrates the uncertainty in fixing a_J resonances. A noticeable difference between Figs. 2a and 2b consists in the prediction of $a_0(1800)$ for $\mu^2=1.1$ GeV^2.

For the 02^{++} states a quadruplet of trajectories arises due to the presence of two waves, ${}^3P_2$ and ${}^3F_2$, and two flavor components, $n\bar{n}$ and $s\bar{s}$. To set $f_2(02^{++})$ mesons on (n,M^2) trajectories with $\mu^2=1.38$ GeV^2 faces a problem, which is seen in Fig. 2c: we cannot fit the experimental data unam-

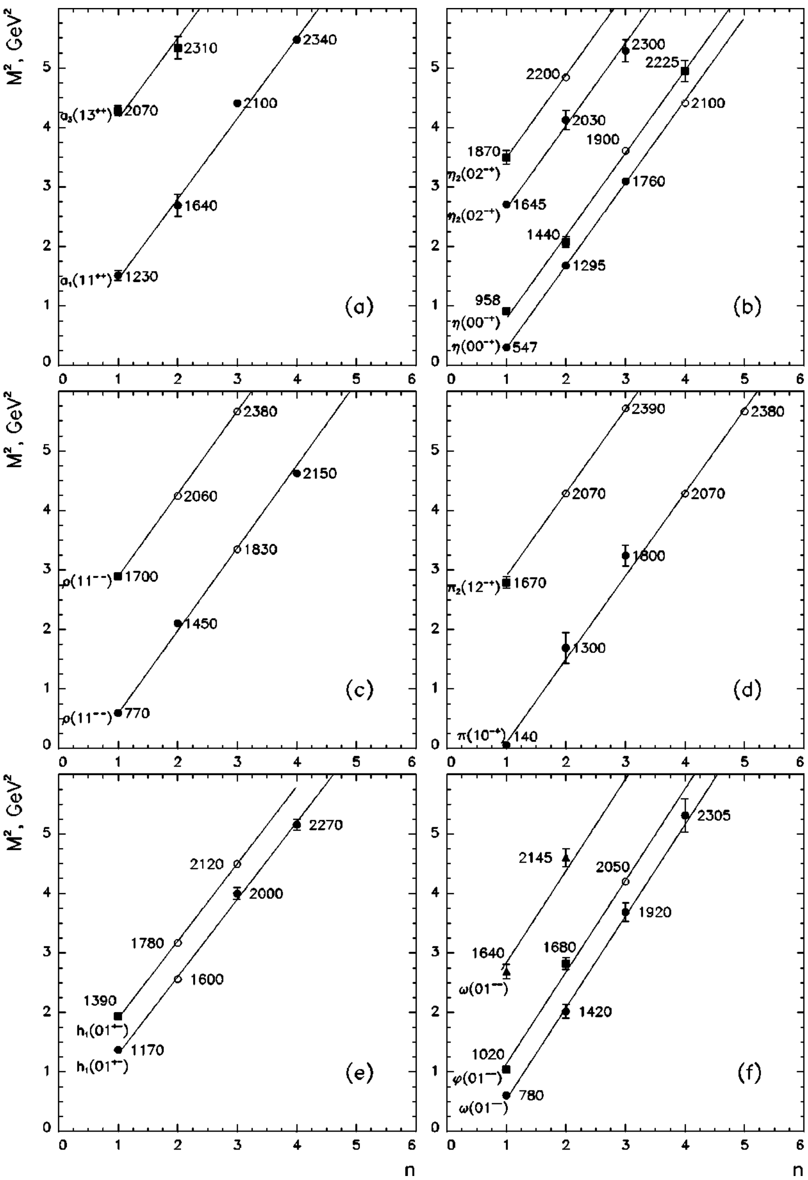

FIG. 1. The (n,M^2) plots for the states: (a) $a_1(11^{++})$ and $a_3(13^{++})$, $\mu^2=1.35\ \mathrm{GeV}^2$; (b) $\eta(00^{-+})$ and $\eta_2(02^{-+})$, $\mu^2=1.39\ \mathrm{GeV}^2$; (c) $\rho(11^{--})$, $\mu^2=1.39\ \mathrm{GeV}^2$; (d) $\pi(10^{-+})$ and $\pi_2(12^{-+})$, $\mu^2=1.39\ \mathrm{GeV}^2$; (e) $h_1(01^{+-})$, $\mu^2=1.30\ \mathrm{GeV}^2$; (f) $\omega(01^{--})/\varphi(01^{--})$, $\mu^2=1.54\ \mathrm{GeV}^2$. Open circles stand for states predicted by the present classification.

biguously. We know definitely two $1^3P_2q\bar{q}$ states which are $f_2(1285)$ and $f_2(1525)$. This establishes masses of other f_2 mesons on these trajectories: they are to be near 1700 MeV, 1940 MeV, 2060 MeV, 2260 MeV, 2390 MeV. The trajectories of $1^3F_2q\bar{q}$ states are located higher, with a gap of the order of $\Delta M^2 \simeq 2.5\ \mathrm{GeV}^2$, which gives mesons with masses around 2050 MeV, 2200 MeV, 2350 MeV. The compilation [7] presents three candidates for f_2 with the mass near 1700 MeV: $f_2(1640)$, $f_J(1710)$, and $f_2(1800)$; the resonance $f_2(1950)$ has been seen in $\pi\pi\pi\pi$ [5]. Simultaneous analysis of the $\pi\pi$, $\eta\eta$ and $\eta\eta'$ spectra [6] gives evidence for $f_2(1910)$, $f_2(2020)$, $f_2(2230)$ and $f_2(2300)$; in the compilation [7], the state $f_2(2150)$ is also under discussion. In the $\phi\phi$ spectra three tensor resonances were seen: $f_2(2010)$, $f_2(2300)$, $f_2(2340)$ [10]. Comparison of the predictions given by Fig. 2c with the observed mesons does not present strong arguments in favor of $\mu^2 \simeq 1.38\ \mathrm{GeV}^2$. The description of data with $\mu^2 \simeq 1.10\ \mathrm{GeV}^2$ looks much more reasonable; see Fig. 2d. Nevertheless, we must admit that the location of all cited f_2 mesons on the trajectories is questionable at the present level of knowledge: the main problem is to distinguish between different states with close masses. To this aim a more sophisticated technique is needed, that is, a simultaneous analysis of available data in the framework of the K-matrix approach or N/D method.

In Fig. 2e the trajectories $f_0(00^{++})$ are displayed: they are doubled due to two flavor components, $n\bar{n}$ and $s\bar{s}$. We do not put the enigmatic σ meson [11–14] on the $q\bar{q}$ trajectory supposing σ is alien to this classification. The broad state $f_0(1530^{+90}_{-250})$ [or $\epsilon(1400)$ in old notation], which is the descendant of the scalar glueball after mixing with the neighboring $q\bar{q}$ states [15,16], is superfluous for the $q\bar{q}$ trajectories and is also not put on the trajectory.

Trajectories $f_0(00^{++})$ in Fig. 2e are drawn for the masses of real resonances. However, in case of scalar/isoscalar $q\bar{q}$ states there is an effect which is specific for 00^{++} wave, that is, a strong mixing of $q\bar{q}$ states due to their overlapping: the

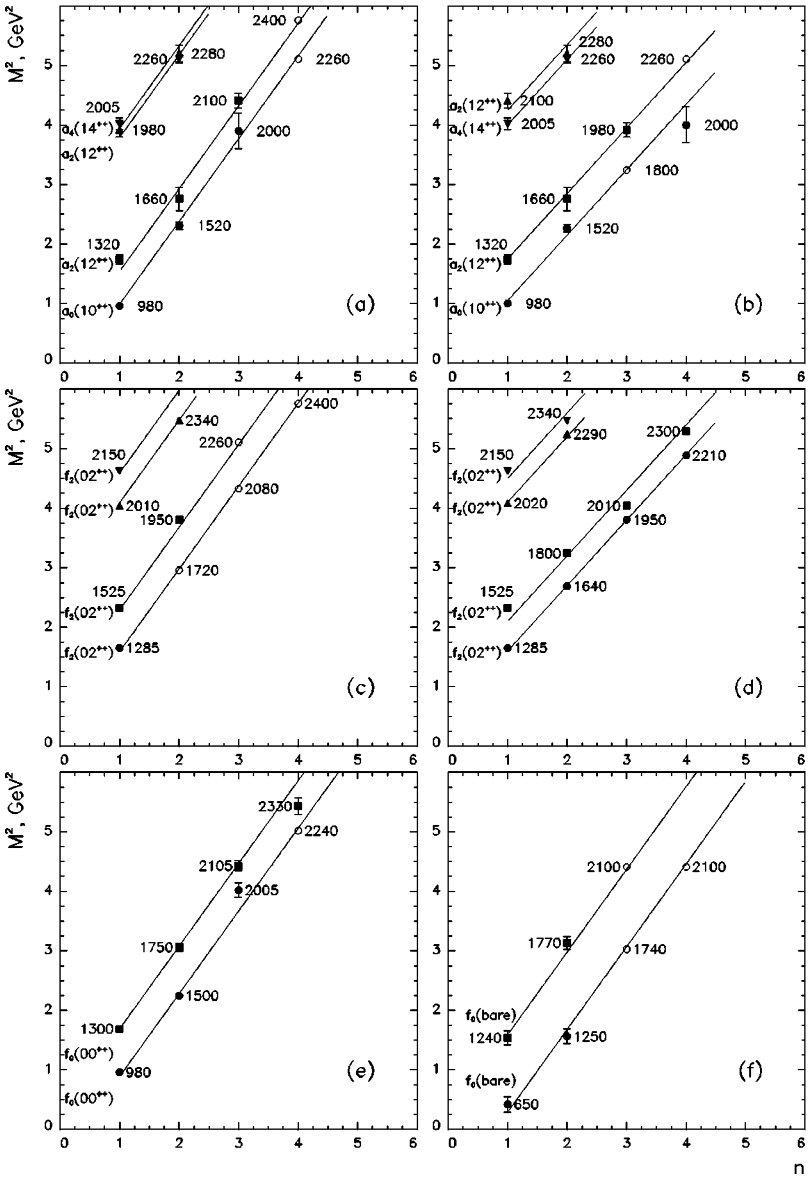

FIG. 2. The (n,M^2) trajectories for the states $a_0(10^{++})$, $a_2(12^{++})$ and $a_4(14^{++})$ with (a) $\mu^2=1.39$ GeV^2 and (b) $\mu^2=1.10$ GeV^2; two variants for the $f_2(02^{++})$ trajectories with the slope parameter (c) $\mu^2=1.39$ GeV^2 and (d) $\mu^2=1.10$ GeV^2. The $f_0(00^{++})$ trajectories for (e) real resonance states ($\mu^2=1.39$ GeV^2) and (f) K matrix pole states ($\mu^2=1.39$ GeV^2). As in Fig. 1, the open circles stand for states predicted by the present classification.

transitions *resonance 1→real mesons→resonance 2* result in a considerable mass shift (detailed discussion may be found in [15,16]). The states ''before mixing'' which respond to K matrix poles were found in [15,16] for two multiplets, 1^3P_0 and 2^3P_0 (these states were denoted as f_0^{bare}). For the K-matrix pole the corresponding trajectories exist, and the problem consists of understanding the dynamics of trajectory deformation for states where the decay channels are switched on. So it is rather instructive to see the location of f_0^{bare} at the (n,M^2) plane: corresponding trajectories are shown in Fig. 2f. One can see a degeneracy of states belonging to two different trajectories; just this degeneracy has enlarged the mixing of f_0 states in the region 1000–1800 MeV. Supposing the linearity of trajectories, we see that a strong mixing of scalar/isoscalar states is very possible at higher masses as well.

The trajectories of the (n,M^2) plots should be complemented by those of (J,M^2) plots: they are shown in Fig. 3. The important point is the leading meson trajectories (π, ρ, a_1, a_2 and P') are known from the study of hadron diffractive processes at $p_{lab}\sim 5-50$ GeV/c (for example, see [17]).

The π-meson trajectories, leading and daughter ones (see Fig. 3a), are linear. The leading trajectory includes $\pi(140)$, $\pi_2(1670)$ and $\pi_4(2350)$, while the daughter one contains $\pi(1300)$ and $\pi_2(2100)$. The other leading trajectories (ρ, η, a_1, a_2, f_2 or P') are also compatible with linear-type behavior:

$$\alpha_X(M^2)\simeq\alpha_X(0)+\alpha'_X(0)M^2. \qquad (3)$$

Parameters for leading trajectories, which are defined by the positions of $q\bar{q}$ states, are as follows:

$$\alpha_\pi(0)\simeq-0.015, \quad \alpha'_\pi(0)\simeq0.72\ \text{GeV}^{-2};$$

$$\alpha_\rho(0)\simeq0.50, \quad \alpha'_\rho(0)\simeq0.83\ \text{GeV}^{-2};$$

$$\alpha_\eta(0)\simeq-0.24, \quad \alpha'_\eta(0)\simeq0.80\ \text{GeV}^{-2};$$

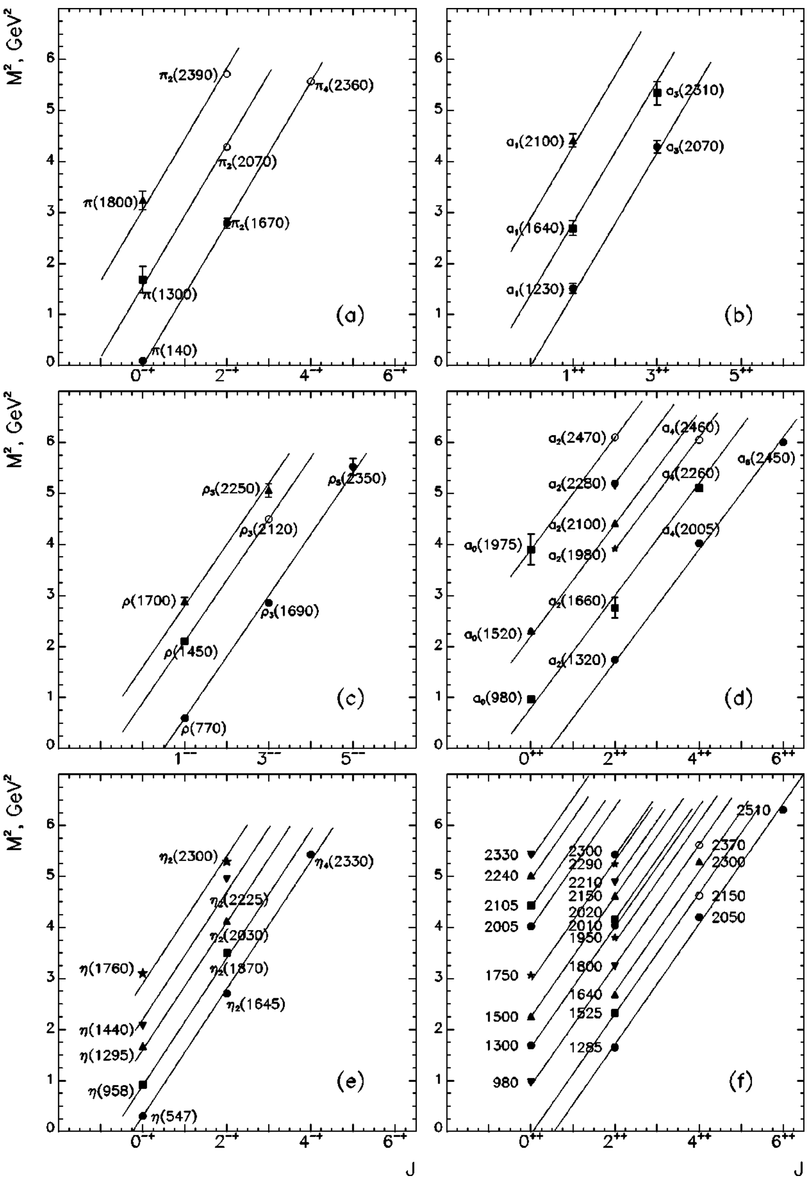

FIG. 3. The (J,M^2) plots for leading and daugther trajectories: (a) π trajectories, (b) a_1 trajectories, (c) ρ trajectories, (d) a_2 trajectories, (e) η trajectories, (f) P' trajectories.

$$\alpha_{a_1}(0)\simeq 0, \quad \alpha'_{a_1}(0)\simeq 0.72 \ \text{GeV}^{-2};$$

$$\alpha_{a_2}(0)\simeq 0.45, \quad \alpha'_{a_2}(0)\simeq 0.91 \ \text{GeV}^{-2};$$

$$\alpha_{P'}(0)\simeq 0.71, \quad \alpha'_{P'}(0)\simeq 0.83 \ \text{GeV}^{-2}. \tag{4}$$

The slopes are nearly the same for all trajectories, and the inverse value of a universal slope, $1/\alpha'_X \simeq 1.25\pm 0.15$ GeV^2, is approximately equal to the slope μ^2 for trajectories on the (n,M^2) plot: $\mu^2\simeq 1/\alpha'_X$.

All daughter trajectories for π (Fig. 3a), a_1 (Fig. 3b), ρ (Fig. 3c), a_2 (Fig. 3d) and η (Fig. 3e) are uniquely determined. In the classification of daughter P' trajectories we have used the variant which corresponds to Fig. 2d.

Concerning P' trajectories (Fig. 3f), one should notice that along the line 0^{++} in the region $M\sim 1500-2000$ the density of $q\bar{q}$ states is lower. This is affected by the presence of the light scalar glueball. In this region the state $f_0(1530^{+90}_{-250})$ exists which is the glueball descendant created after mixing with the nearest $q\bar{q}$ neighbors [15,16]. Because of that, the lower density of $00^{++}q\bar{q}$ levels near 1500–1800 MeV does not look eventual: the extra state (gluonium) being mixed with the $q\bar{q}$ state repulses the $q\bar{q}$ levels.

We do not discuss in detail the K meson sector: experimental information in this sector is not sufficient for a reliable analysis. Let us, for example, attend to states where the doubling of trajectories is absent, that is, pseudoscalar and scalar kaons. The Particle Data Group refers to a possible existence of two excited 0^- states [7]: $K(1400-1460)$ and $K(1830)$. Together with $K(500)$, these states may be placed on the linear (n,M^2) trajectory with $\mu^2\simeq 1.55$ GeV^2. For scalar kaons the T matrix analysis of the $K\pi$ spectrum gives two states [18], $K_0(1430\pm 10)$ and $K_0(1950\pm 30)$ which correspond to the trajectory with $\mu^2\simeq 1.75$ GeV^2. Meanwhile the K matrix reanalysis [19] of the data gives either $K_0(1415\pm 30)$ and $K_0(1820\pm 40)$ for the two-pole solution (trajectory with $\mu^2\simeq 1.30$ GeV^2) or $K_0(998\pm 15)$,

$K_0(1445\pm45)$ and $K_0(1815\pm25$ for the three-pole solution (linear trajectory with $\mu^2\simeq1.15$ GeV^2). The trajectory setting other kaon states is more uncertain because of the problem of their multiplet identification.

In conclusion, meson states fit to linear trajectories at the (n,M^2) and (J,M^2) plots with sufficiently good accuracy. The linear behavior of $q\bar{q}$ trajectories at large M^2 should facilitate the $q\bar{q}$ systematizing which is a necessary step in the identification of extra (exotic) states.

We thank Ya.I. Azimov, D.V. Bugg, L.G. Dakhno, G.S. Danilov, S.A. Kudryavtsev, L. Montanet, V.A. Nikonov, and A.A. Yung for useful discussions. This work was supported by the RFFI grant 98-02-17236.

[1] A.V. Anisovich *et al.*, Phys. Lett. B **452**, 187 (1999).
[2] C.A. Baker *et al.*, Phys. Lett. B **449**, 114 (1999).
[3] A.V. Anisovich *et al.*, Phys. Lett. B **452**, 173 (1999).
[4] A.V. Anisovich *et al.*, Phys. Lett. B **452**, 180 (1999).
[5] WA102 Collaboration, D. Barberis *et al.*, Phys. Lett. B **474**, 423 (2000).
[6] A.V. Anisovich *et al.*, Nucl. Phys. **A651**, 253 (1999).
[7] Particle Data Group, C. Caso *et al.*, Eur. Phys. J. C **3**, 1 (1998).
[8] A.V. Anisovich *et al.*, ''Resonances in $p\bar{p}\rightarrow\omega\eta$ from 600 to 1940 MeV/c,'' Phys. Lett. B (to be published).
[9] V.V. Anisovich *et al.*, ''The two-pion spectra for the reaction $\pi^-p\rightarrow\pi^0\pi^0n$ at 38 GeV/c pion momentum and combined analysis of the GAMS, Crystal Barrel and BNL data,'' Phys. At. Nucl. (to be published), hep-ph/9711319.
[10] A. Etkin *et al.*, Phys. Lett. B **201**, 568 (1988).
[11] S. Narison, Nucl. Phys. **B509**, 312 (1998).
[12] M.R. Pennington, *Riddle of the scalars: Where is the σ?*, Frascati Physics Series Vol. XV (1999), p. 95.
[13] L. Montanet, *What do we know about σ?*, Frascati Physics Series Vol. XV (1999), p. 619.
[14] V.V. Anisovich and V.A. Nikonov, ''The low-mass σ-meson,'' hep-ph/9911512 (1999).
[15] V.V. Anisovich, Yu.D. Prokoshkin, and A.V. Sarantsev, Phys. Lett. B **389**, 366 (1996); A.V. Anisovich, V.V. Anisovich, Yu.D. Prokoshkin, and A.V. Sarantsev, Z. Phys. A **357**, 123 (1997); A.V. Anisovich, V.V. Anisovich, and A.V. Sarantsev, Phys. Lett. B **395**, 123 (1997); Z. Phys. A **359**, 173 (1997).
[16] V.V. Anisovich, D.V. Bugg, and A.V. Sarantsev, Phys. Rev. D **58**, 111503 (1998).
[17] P.D.B. Collins, *An Introduction to Regge Theory and High Energy Physics*, Cambridge University Press, Cambridge, England, (1975); V.V. Anisovich, M.N. Kobrinsky, J. Nyiri, and Yu.M. Schabelski, *Quark Model and High Energy Collisions* (World Scientific, Singapore, 1985), Chap. 2.
[18] D. Aston *et al.*, Nucl. Phys. **B296**, 493 (1988).
[19] A.V. Anisovich and A.V. Sarantsev, Phys. Lett. B **413**, 137 (1997).